



HAL
open science

Tracing Sediment Sources Using Mid-infrared Spectroscopy in Arvorezinha Catchment, Southern Brazil

Tales Tiecher, Laurent Caner, Jean Paolo Gomes Minella, O. Evrard, Leslie Mondamert, Jérôme Labanowski, Danilo dos Santos Rheinheimer

► **To cite this version:**

Tales Tiecher, Laurent Caner, Jean Paolo Gomes Minella, O. Evrard, Leslie Mondamert, et al.. Tracing Sediment Sources Using Mid-infrared Spectroscopy in Arvorezinha Catchment, Southern Brazil. *Land Degradation and Development*, 2017, 28 (5), pp.1603-1614. 10.1002/ldr.2690 . hal-01940766

HAL Id: hal-01940766

<https://hal.science/hal-01940766>

Submitted on 28 May 2020

HAL is a multi-disciplinary open access archive for the deposit and dissemination of scientific research documents, whether they are published or not. The documents may come from teaching and research institutions in France or abroad, or from public or private research centers.

L'archive ouverte pluridisciplinaire **HAL**, est destinée au dépôt et à la diffusion de documents scientifiques de niveau recherche, publiés ou non, émanant des établissements d'enseignement et de recherche français ou étrangers, des laboratoires publics ou privés.

1 TRACING SEDIMENT SOURCES USING MID-INFRARED SPECTROSCOPY IN
2 ARVOREZINHA CATCHMENT, SOUTHERN BRAZIL

3
4 Tales Tiecher^{1*}, Laurent Caner², Jean Paolo Gomes Minella³, Olivier Evrard⁴, Leslie
5 Mondamert⁵, Jérôme Labanowski⁵, Danilo Rheinheimer dos Santos³

6
7 ¹ Universidade Federal do Rio Grande do Sul (UFRGS), Department of Soil Sciences, Bento Gonçalves Avenue
8 7712, CEP 91540-000, Porto Alegre, RS, Brazil

9 ² Université de Poitiers, IC2MP-HydrASA UMR 7285, 7 rue Albert Turpain, TSA51106, 86073, Poitiers, France

10 ³ Universidade Federal de Santa Maria, Department of Soil Science, 1000 Avenue Roraima, 97105-900, Santa
11 Maria, Rio Grande do Sul State, Brazil

12 ⁴ Laboratoire des Sciences et de l'Environnement, UMR 8212 (CEA/CNRS/UVSQ), Université Paris-Saclay,
13 Domaine du CNRS, Avenue de la Terrasse, 91198 Gif-sur-Yvette Cedex, France

14 ⁵ Université de Poitiers, IC2MP-Equipe Eaux Géochimie Santé E1UMR 7285, 1 rue Marcel Dore, B1, 86022,
15 Poitiers, France

16 * Corresponding author: Tales Tiecher. E-mail: tales.tiecher@ufrgs.br

17
18 ABSTRACT

19 The widespread adoption of the sediment fingerprinting approach to guide catchment management
20 has been limited by the cost and the difficulty to prepare and process samples for geochemical and
21 radionuclide analyses. Spectral properties have recently been shown to provide a rapid and cost-
22 efficient alternative for this purpose. The current research objective was (i) to quantify the
23 sediment source contributions in a 1.19-km² rural catchment of Southern Brazil by using mid-
24 infrared (MIR) spectroscopy, and (ii) to compare these results with those obtained with
25 geochemical approach and near-infrared (NIR) and ultraviolet-visible (UV-VIS) spectroscopy
26 methods. The sediment sources to discriminate were cropland surface ($n=20$), unpaved roads
27 ($n=10$) and stream channel banks ($n=10$). Twenty-nine suspended sediment samples were
28 collected at the catchment outlet during nine significant flood events. The sources could be
29 distinguished by MIR spectroscopy. Cropland and channel bank sources mainly differed in their
30 clay mineral contents, but their similar organic matter content complicated the MIR-model
31 predictions. Unpaved road contributions were discriminated from the other sources by their lower
32 organic carbon content. When the results of the current research based on MIR spectroscopy are
33 compared to those obtained using other sediment fingerprinting approaches, based on
34 geochemistry and NIR and UV-VIS spectroscopy, an overestimation of channel banks contribution
35 and an underestimation of cropland and unpaved road contributions is found. These results suggest
36 that MIR spectroscopy can provide a useful tool that is non-destructive, rapid and cheap for tracing
37 sediment sources in rural catchments and for guiding the implementation of soil and water
38 conservation measures.

39
40 KEY WORDS: soil erosion, sediment fingerprinting, spectral properties, suspended sediment,
41 rapid and cost-efficient tracers.

INTRODUCTION

Intensification of agriculture for increasing food production has led to the degradation of soil and water resources during the last several decades (Comino *et al.*, 2015; Erkossa *et al.*, 2015; Seutloali and Beckedahl, 2015; Taguas *et al.*, 2015). Modern and intensive agricultural practices expose the soil to the erosion and accelerate the transfer of sediment to the lower parts of landscape (Minella *et al.*, 2014) and into water bodies, along with contaminants such as pesticides (Magnusson *et al.*, 2013; Yahia and Elsharkawy, 2014) and phosphorus (Poulenard *et al.*, 2008; Dodd *et al.*, 2014; Dodd and Sharpley, 2015). In agricultural catchments with high runoff coefficients and sediment yields, as in Southern Brazil, erosion process needs to be controlled to prevent an irreversible degradation of soil and water quality (Didoné *et al.*, 2015; Merten *et al.*, 2015). In order to mitigate these problems at the catchment scale, it is first required to have information on the respective contributions of the potential sources of sediment to the river.

Accordingly, the sediment fingerprinting approach quantifies the contribution of non-point sediment sources through the use of a range of natural tracers combined with rigorous statistical modeling techniques. This tool is very useful to assist local managers in developing strategies for remediating river siltation and pollution in catchments (Walling and Woodward, 1995; Davis and Fox, 2009; D'Haen *et al.*, 2012; Haddadchi *et al.*, 2013; Koiter *et al.*, 2013). However, the wider application of this technique by local managers is complicated by the difficulty accessing the conventional physicochemical analysis techniques, their cost, and the necessity to collect sufficient material in the rivers to conduct these (generally) destructive measurements (Cooper *et al.*, 2014).

Spectroscopic reflectance is a low-cost and non-destructive alternative methods that can be carried out very quickly on dried sieved samples to assess various physical, chemical and biological properties of soils (McBratney *et al.*, 2006; Viscarra Rossel *et al.*, 2006). In this sense, Poulenard *et al.* (2009) developed a first attempt to use Diffuse Reflectance Infrared Fourier Transform Spectroscopy (DRIFTS) to fingerprint sediment sources in catchments. The method was successfully used to discriminate and predict the contributions of topsoil and channel sources (Poulenard *et al.*, 2009) and soils developed on different substrates to sediment (Poulenard *et al.*, 2012). In addition, both studies confirmed that these properties remained conservative during a time period consistent with the duration of the study (i.e., min. 1 month), and this is a prerequisite for a property to be used as a tracer.

In the last years, several studies using spectroscopic method have been developed worldwide to trace sediment sources. Visible (VIS) and near-infrared (NIR) reflectance was tested in the French Alps (Legout *et al.*, 2013), Luxemburg (Martínez-Carreras *et al.*, 2010a, 2010b, 2010c), Spain (Brosinsky *et al.*, 2014a, 2014b), Ethiopia (Verheyen *et al.*, 2014), the Eastern Cape

76 of South Africa (Pulley and Rowntree, 2015), United Kingdom (Collins *et al.*, 2014), and southern
77 Brazil (Tiecher *et al.*, 2015, 2016). Besides, some of these studies showed a good agreement
78 between the results obtained with the spectroscopic method and those provided by the
79 conventional fingerprinting approach based on geochemical properties (Martínez-Carreras *et al.*,
80 2010c; Legout *et al.*, 2013; Verheyen *et al.*, 2014; Tiecher *et al.*, 2015, 2016). Near-infrared
81 spectroscopy have proved to be a valuable tool to trace sediment originating from different land
82 uses [e.g. badland, forest/grassland, others – Brosinsky *et al.* (2014a, 2014b); landslide, cropland,
83 grazing land – Verheyen *et al.* (2014); cropland, unpaved road, stream channels – Tiecher *et al.*
84 (2016)], parent material [black marls, limestones, molasses – Legout *et al.* (2013)]. However, some
85 of these studies warned that these technique may not necessarily work in all catchments because
86 of the risks of significant non-conservative tracer behaviour of organic molecular structures
87 (Collins *et al.*, 2014) or high-soluble minerals, such as gypsum (Legout *et al.*, 2013).

88 To the best of our knowledge, there are very few studies using spectroscopic measurements
89 in the mid-infrared (MIR) region for sediment tracing (Poulenard *et al.*, 2009, 2012; Evrard *et al.*,
90 2013). Nevertheless, several studies have proved that the MIR is more suitable than the VIS or
91 NIR due to the higher incidence of spectral bands in this region as well as the higher intensity and
92 specificity of the signal (Viscarra Rossel *et al.*, 2006; Reeves, 2010; Xie *et al.*, 2011; Soriano-
93 Disla *et al.*, 2014) Although Evrard *et al.* (2013) found similar results with conventional and
94 alternative tracing methods, it showed that the MIR spectroscopy, like NIR spectroscopy, is very
95 sensitive to the organic matter content in sediment. This technique should therefore be applied in
96 other environmental contexts in order to test the general applicability of MIR spectroscopy
97 methods for sediment fingerprinting. Moreover, to date, there has been no attempt to compare the
98 use of spectroscopy for tracing sediment sources in the different ranges of the electromagnetic
99 spectrum, such as MIR, NIR, and ultraviolet-VIS (UV-VIS) infrared.

100 To this end, the objectives of the current research were (i) to evaluate the sediment source
101 contributions in a subtropical rural catchment of southern Brazil using this alternative MIR
102 spectroscopy-based method, and (ii) to compare these results with those obtained by the
103 conventional fingerprinting approach based on geochemical properties, and those obtained by
104 NIR- and UV-VIS-spectroscopy based methods (data published in Tiecher *et al.* 2015, 2016).
105 Then, the physicochemical basis of the source discrimination provided by MIR spectroscopy
106 properties was discussed.

107

108

MATERIAL AND METHODS

109 *Study catchment*

110 The Arvorezinha catchment (Fig. 1) covers a surface area of 1.19 km² and it is located on
111 the upper north-eastern edge of the Rio Grande plateau, in Rio Grande do Sul, the southernmost
112 state of Brazil (Fig. 1). The Arvorezinha catchment is located in the headwaters of the Taquari
113 River, a tributary of the Jacuí River, which is one of the major water bodies in the region. The
114 average channel slope is 9%. The time to peak for flood hydrographs recorded at the outlet
115 typically ranges from 20 to 50 min. The area is mainly underlain by extrusive igneous rocks
116 (rhyodacite). The altitude ranges from 560 to 740 m. Hillslopes on top of the catchment have an
117 undulating topography (7% slope), whereas they may be classified as rolling (>15%) and short in
118 the middle and lower parts of the catchment (Soil Survey Division Staff, 1993). According to the
119 Köppen classification, the climate is classified as subtropical super humid mild (Cfb type) with
120 warm summer and the absence of dry season. Mean annual rainfall is 1605 mm. The erosivity
121 index (EI30) calculated from 40 years of historical data is 6540 MJ mm ha⁻¹ year⁻¹, which can be
122 considered as moderate to strong (Argenta *et al.*, 2001).

123 Soil types in the catchment according to World Reference Base for soil Resources (WRB)
124 (IUSS Working Group WRB, 2007) and determined from a detailed soil classification survey
125 (1:5000) are Acrisols (57%), Cambisols (33%) and Leptosols (10%). Acrisols are mainly found in
126 upper parts of the catchment, and they are characterized by an abrupt texture change between
127 horizons A and B, leading to a reduction of infiltration in the low permeable argic B horizon
128 because of its higher clay content. Isolated spots of Cambisols are found in areas dominated by
129 Acrisols and/or Leptosols. The Leptosols occur in the lower parts of the catchment, where the
130 relief is the steepest. Land uses are not related to the soil types. Therefore, samples of potential
131 sediment sources were collected on soils representative of all soil types found in the catchment,
132 respecting the proportion of the surface area covered by each soil type.

133 There is no urban area in Arvorezinha catchment. It is inhabited by a local rural community
134 (Cândido Brum) including 16 families growing tobacco in small farms (7–10 ha). Tobacco is
135 cultivated under minimum tillage (31.2% of the catchment surface area) or under conventional
136 ploughing (13.5%). Other land uses in the catchment (55.3%) are native forest, fallow, areas
137 afforested with eucalyptus and grassland (Barros *et al.*, 2014).

138 139 *Source material sampling*

140 Three main sediment sources types were identified during previous research (Minella *et*
141 *al.*, 2008, 2009b), namely: (i) surface of cropland, (ii) unpaved roads and (iii) stream channel
142 banks. Areas under pasture, fallow and forest were not included as a potential source because
143 previous research showed their low sensitivity to erosion (Minella *et al.*, 2009a). The samples of

144 potential source material were collected using non-metallic trowels in the uppermost layer (0–0.05
145 m) of the cropland surface ($n=20$) and unpaved roads ($n=10$), and on exposed sites located along
146 the main river channel network ($n=10$) by scraping the surface of river banks. Care was taken to
147 avoid sampling material recently deposited on the channel bank. Each sample was composed of
148 10 sub-samples collected in the vicinity of the sampling point in order to obtain representative
149 source material. Sampling points were concentrated in sites sensitive to erosion and potentially
150 connected to the river network. Sediment source sampling was performed to cover the entire range
151 of soil types found in the catchment.

152

153 *Suspended sediment sampling*

154 Twenty-nine suspended sediment samples were collected at various stages (rising,
155 recession limbs) during nine significant floods between October 2009 and July 2011 (Maier,
156 2013). A large volume of water (120 to 200 liters) was collected manually on a footbridge built at
157 the outlet. Each bulk water sample was centrifuged in a continuous flow centrifuge (Alfie-500 Alfa
158 Laval) to concentrate sediment samples for subsequent spectroscopy analysis.

159

160 *Source material and sediment analysis*

161 All the source material and sediment samples were oven-dried at 50°C, gently
162 disaggregated using a pestle and mortar, and passed through a 63 μm mesh prior to laboratory
163 analyses to compare similar particle size fractions in all the samples. Mid-infrared (MIR) diffuse
164 reflectance spectra were recorded in the 400–4000 cm^{-1} region using a Nicolet 510- FTIR
165 spectrometer (Thermo Electron Scientific, Madison, WI, USA) in reflection mode with a 2 cm^{-1}
166 resolution and 100 co-added scans per spectrum. The spectrometer was continuously purged with
167 dry CO_2 -depleted air. Care was taken when adding the samples into the sample port to avoid
168 differences in sample packing and surface smoothness.

169

170 *Sediment source discrimination based on MIR-spectroscopy*

171 Sediment source discrimination was performed using the second-derivative of MIR spectra
172 of the source samples. Using the second-derivative avoids differences in baseline positions and
173 removing the small differences that may arise from uncontrolled sources of variation (e.g. sample
174 packaging). Derivative treatment not only reduces scattering effects but also increases the
175 resolution of spectral peaks of both mineral (Scheinost *et al.*, 1998) and organic (Fernández-Getino
176 *et al.*, 2010) components.

177 The band 2360–2325 cm^{-1} of MIR spectra corresponds to the CO_2 molecule vibrations.
178 Even purging the entire analysis chamber with CO_2 -free gas, it is possible that some CO_2 has been
179 trapped between the soil particles. For this reason, in order to avoid any CO_2 (gas) interference in
180 MIR spectra, the wavelengths from 2400–2300 cm^{-1} were removed, and statistical analyses were
181 performed on wavelengths in the ranges of 3800–2400 cm^{-1} and 2300–650 cm^{-1} .

182 Data obtained from the MIR spectroscopy consists of a continuous spectrum with a large
183 number of variables (intervals of 2 cm^{-1} = 1583 wavenumbers) for a set of 40 sediment source
184 samples. A Principal Component Analysis (PCA) was performed to reduce the number of variables
185 without losing significant information. PCA was performed using the R package “ade4” (R-
186 project.org). Then, a Discriminant Function Analysis (DFA) in backwards mode was conducted
187 on the scores obtained from the PCA. At each step, the principal component (PC) which minimized
188 the overall Wilks' Lambda was entered. Maximum significance of F to enter a principal component
189 (PC) was 0.01. Minimum significance of F to remove a PC was 0.01. DFA was performed using
190 STATISTICA software.

191

192 *Sediment source quantification using the MIR-spectroscopy approach*

193 The individual samples representative of each sediment source (i.e. 20 samples of cropland
194 surface, 10 samples of unpaved roads, and 10 samples of stream channel banks) were mixed in
195 equal proportions at the laboratory to prepare a unique reference sample for each source. Then, the
196 three reference source samples were mixed in different weight proportions to obtain 48 composites
197 with different source material ratios as displayed in Fig. 2. MIR spectra were obtained for each
198 mixture.

199 Relationships between MIR spectra (x variate) and the corresponding weight contribution
200 of each sediment source (y variate) were analyzed using partial least squares regressions (PLSR).
201 The composites samples were randomly chosen to build the model. Thirty-six mixed samples were
202 used to develop the calibration models and the remaining 12 mixed samples were used for model
203 validation. The number of components providing the lowest predictive standard error was used.
204 PLSR was performed using STATISTICA software.

205 The predictive performance of the models was evaluated by calculating several standard
206 indicators such as the root mean square error of calibration (RMSEC), the root mean square error
207 of cross-validation (RMSECV), the root mean square error of prediction (RMSEP), the ratio
208 RMSECV to standard deviation (RPD) and the coefficient of determination R^2 obtained when
209 comparing predicted values with reference data. The uncertainty associated with the prediction
210 was estimated by the confidence interval (95%) of prediction calculated by the regression of

211 predicted values against reference data. Three independent MIR-PLSR models were constructed
212 to estimate the proportion of sediment supplied by the three sources. MIR spectra of suspended
213 sediment were then introduced into these MIR-PLSR models to estimate the contribution of each
214 sediment source and the associated uncertainty.

215

216

RESULTS AND DISCUSSION

217

Source discrimination

218

219

220

221

222

223

224

225

226

227

228

229

230

231

232

233

234

235

236

237

238

239

240

241

242

243

244

MIR spectra of the <63 μm fractions of suspended sediment and sediment source samples were very similar, and 16 spectral features were observed in all spectra (Fig. 3a and Table 1). In order to simplify the interpretation, the spectral features were grouped according to the main soil constituents, namely Soil Clay Minerals (SCM – kaolinite [Kt], smectite [Sm], mica [Mc], hydroxy-interlayered vermiculite [HIV], gibbsite [Gb]), quartz (Qz), and organic compounds (OC) (Viscarra Rossel and Behrens, 2010; Madejová *et al.*, 2011; Terra, 2011; Yang and Mouazen, 2012). Spectral feature 1 at 3695 cm^{-1} corresponds to OH stretching (ν_{1a}) of Kt. Spectral features 2, 12, 13, 14 and 16 at 3620, 1115, 1020, 915 and 698 cm^{-1} correspond to SCM (Table 1). Spectral features 3 and 4, measured at 2930 and 2850 cm^{-1} , correspond to C–H stretching of aromatic and aliphatic organic compounds, respectively. Spectral features 5, 6, and 7 at 1990, 1870 and 1785 cm^{-1} correspond to Si–O stretching bands of Qz. Spectral features 8 and 15 at 1630 and 808 cm^{-1} correspond to both SCM and Qz; features 9 and 10 at 1530 and 1340 cm^{-1} correspond to both OC and Qz; feature 11 at 1160 cm^{-1} correspond to both OC and SCM (Table 1).

The potential of the spectroscopy method to discriminate sediment sources was analyzed based on the scores obtained from the PCA. The scores of 39 principal components (PC) obtained in the PCA were then entered in the DFA (PC-DFA model) where six PCs were selected. These six PCs together explained 70.8% of the total variation obtained from the 39 PCs. In the DFA, the final Λ^* value was 0.0342 (Table 2), meaning that 96.6% of variation included in these six PCs was due to differences between sediment sources, and only 3.4% of the variation was due to intra-source differences. The PC-DFA model correctly classified 97.5% of the sediment source samples with an average uncertainty of 3.426% (Table 2). The square Mahalanobis distance between channel banks and cropland surface was smaller (18.4) than the distance between these sources and unpaved roads (channel banks vs. unpaved roads = 38.7, cropland surface vs. unpaved roads = 29.7) (Fig. 4). Nonetheless, the distances between sediment sources remained systematically significant ($P < 6.5\text{E-}09$) (Table 2).

Partial last-square models based on MIR spectroscopy

245 MIR-PLSR model performance is given in Table 3. Four components were used to
246 construct MIR-PLSR models. Correlations between actual and predicted proportions were very
247 high, with R^2 values close to 1 for the three independent MIR-PLSR models (Fig. 5). RPD values
248 higher than 2 indicate robust models of high quality (Chang *et al.*, 2001). In the current research,
249 all the independent MIR-PLSR models showed RPD values higher than 10, indicating a good
250 predictability. Moreover, the average difference between predicted and actual values on the
251 calibration dataset measured by the RMSEP parameter was always lower than 4.7%.

252 Regions of the MIR spectra providing the best discrimination between the sediment sources
253 are shown in Fig. 3. Fig. 3b display the second-derivative of MIR spectra of all the three sediment
254 sources. To facilitate the visualization of differences in the spectral features, the differences
255 between the second-derivatives of each source are shown in Fig. 3c, d, e. These figures show a
256 greater variation between the unpaved roads vs. cropland surface (Fig. 3d) and unpaved roads vs.
257 channel banks (Fig. 3e) than between cropland surface vs. channel banks (Fig. 3c).

258 Spectral features at 2930 and 2850 cm^{-1} corresponding to C–H stretching of aromatic and
259 aliphatic functional compounds, respectively, provided a better discrimination of unpaved roads
260 (Fig. 3d, e). In contrast, they did not vary between cropland surface and channel banks (Fig. 3c).
261 The same interpretation can be made for the spectral features found at 1160 cm^{-1} (OC + SCM) and
262 at 1530 and 1340 cm^{-1} (OC + Qz). This difference is likely due to the lower content of TOC in
263 unpaved roads ($12.0 \pm 5.5 \text{ g C kg}^{-1}$, data not shown) compared to cropland surface and channel
264 banks (20.5 ± 6.6 and $21.3 \pm 3.1 \text{ g C kg}^{-1}$, respectively, data not shown). Moreover, a higher
265 abundance of 2:1 clay minerals and a lower quantity of Qz in the unpaved roads compared to the
266 cropland and channel banks may have contributed to the better discrimination of unpaved roads
267 with the spectral features 1, 2, 12, 13, 14 and 16 (SCM), and the spectral features 5, 6 and 7 (Qz).
268 Thus, the combined effect of differences in mineral composition and organic matter content
269 resulted in the lowest predictive error ($\pm 2.8\%$) for the MIR-PLSR models built for unpaved roads
270 (Fig. 5b and Table 3), and in the correct classification of 100% of the road samples (Table 2). As
271 a result of the much more similar mineral and organic compositions of cropland and channel bank
272 sources, the predictive errors were higher (5.9 for cropland and 5.1% and channel banks) than
273 those obtained for unpaved roads (2.8%) (Table 3). However, errors associated with all MIR-PLSR
274 models remained far below the 15%-threshold, which was considered as ‘acceptable’ in previous
275 sediment fingerprinting studies (Collins and Walling, 2002).

276

277 *Source contribution to sediment*

278 The uncertainty of MIR-PLSR model predictions remained very low (see the 95%
279 confidence intervals on Fig. 5, with a mean of 4.6% for the three sediment sources) (Table 3).
280 Source contributions were very variable from one event to the next, with a dominance in similar
281 proportions of cropland surface (mean: $42 \pm 27\%$; Fig. 6) and channel banks (mean: $43 \pm 19\%$; Fig.
282 6), and a much lower contribution of unpaved roads (mean: $16 \pm 10\%$; Fig. 6). When these results
283 are compared to those obtained by Tiecher *et al.* (2015) using conventional sediment fingerprinting
284 based on geochemical properties, the cropland contribution was clearly underestimated by the
285 spectroscopic method, whereas channel bank contribution was overestimated (Fig. 6). In contrast,
286 the contribution of unpaved roads calculated by both methods remained very similar (Fig. 6.).

287 When compared to the results obtained with other sediment fingerprinting approaches, such
288 as those based on elemental geochemistry (Tiecher *et al.*, 2015), ultraviolet-visible (UV-VIS)
289 (Tiecher *et al.*, 2015), and near-infrared (NIR) properties (Tiecher *et al.*, 2016), the results found
290 with MIR spectroscopy showed an overestimation of channel bank contribution and an
291 underestimation of cropland and unpaved road contributions (Fig. 6). Moreover, MIR-PLSR
292 model predictions showed the highest difference in source contributions compared to those
293 obtained with geochemical properties (Fig. 7). Although NIR-PLSR predictions were the closest
294 to those obtained with the geochemical approach, there was no significant correlation between the
295 methods (Table 4). UV-VIS-PLSR showed an intermediate behaviour, with slight variations in
296 source contributions compared to those obtained with the geochemical approach. In addition, UV-
297 VIS predictions were well correlated to MIR predictions for all sediment sources and showed a
298 significant correlation with results of the geochemical approach for cropland and unpaved roads
299 (Table 4).

300 A strong positive correlation ($p = 0.001$, $r = 0.57$) was found between the cropland surface
301 contributions calculated by both approaches (Table 4 and Fig. 7). The contribution of unpaved
302 road estimated by MIR-PLSR models was poorly correlated to the contribution obtained by
303 geochemical approach ($p = 0.108$, $r = 0.30$, Table 4). This type of relationship was not observed
304 for channel banks. Moreover, the unpaved road contribution predicted by the spectroscopic method
305 was found to be negatively correlated with the total organic carbon content in suspended sediment
306 (Fig. 8). This result demonstrates that the mid-infrared signature and the results of MIR-PLSR
307 models were impacted by the low organic carbon content found in deep soil horizons
308 corresponding to unpaved road material, which may explain why unpaved road predictions were
309 very similar for both methods (Fig. 6). When assuming that the sediment source contributions
310 provided by the conventional fingerprinting method based on geochemistry are correct and
311 reflecting the ground truth, results of the current research demonstrate that the analysis of the MIR

312 region of the electromagnetic spectrum provided less accurate results than the NIR and UV-VIS
313 regions. This is likely due to the higher sensitivity of MIR to organic matter, as observed in several
314 other studies (Viscarra Rossel *et al.*, 2006; Reeves, 2010; Xie *et al.*, 2011; Soriano-Disla *et al.*,
315 2014).

316

317 *Physicochemical basis of the source discrimination provided by MIR spectroscopy*

318 In the Arvorezinha catchment, the discrimination between sediment sources by using MIR
319 spectroscopy was possible due to differences in both organic carbon content and in mineralogical
320 composition between sources. It has been demonstrated that the signatures of different organic
321 compounds in the mid-infrared region can be very useful to discriminate topsoils (relatively rich
322 in organic matter) and deeper horizons and gully material depleted in organic matter (Poulenard
323 *et al.* 2009; Evrard *et al.* 2013). However, in certain conditions, the high sensitivity of mid-infrared
324 spectra to the organic carbon content can become problematic. In one of the Mexican catchments
325 investigated by Evrard *et al.* (2013), the source predictions based on the spectroscopic method
326 greatly differed from those provided by the classical sediment fingerprinting method based on
327 geochemical properties because one source of soluble organic matter delivered by anthropogenic
328 activities (excess of cow dung) caused an enrichment of carbon in sediments, leading to an
329 overestimation of the contribution of surface soil.

330 In Arvorezinha, unpaved roads are composed of subsurface material as these areas have
331 been severely eroded during the last several decades. This process explains the lower organic
332 carbon content found in unpaved roads compared to that measured in cropland surface and channel
333 bank samples, leading to a better discrimination of the former source (see Mahalanobis distances
334 in Table 2). The higher abundance of 2:1 clay minerals in the unpaved road samples is likely due
335 to the fact that most of the soils in Arvorezinha catchment are Acrisols (~57% of the total area).
336 These soils are characterized by the migration of clays in depth, forming a clay-enriched textural
337 B subsurface horizon. The higher abundance of 2:1 clay minerals in unpaved roads is due to the
338 selective eluviation of smectite compared to other sources, which also contributed to the better
339 discrimination of unpaved roads samples. In contrast, the discrimination between cropland surface
340 and channel banks, was complicated by their similar contents and composition in organic carbon.
341 They only differed by their different proportions in mineral components, such as the higher
342 proportion of Qz and the lower content of 2:1 clay minerals in cropland compared to channel
343 banks.

344 It is well known that unpaved rural roads contribute significantly to soil loss in agricultural
345 catchments despite representing a small fraction of watershed-occupied areas (Cao *et al.*, 2015).

346 Despite the low contribution of unpaved roads to sediment obtained in this study ($16\pm 10\%$), they
347 represent perennial landscape features, and their construction should therefore be planned in the
348 framework of integrated soil erosion control programs. The high soil erosion and sediment yield
349 rates in unpaved roads should be taken into account when designing and constructing road and
350 railway cuts, because it is very important for infrastructure maintenance, as well as for soil
351 formation, water protection, vegetation establishment and controlling land degradation (Seutloali
352 and Beckedahl, 2015; Navarro-Hevia *et al.*, 2016). Moreover, unpaved road material can also
353 contain considerable amounts of heavy metals like Pb, Cu, Cd, and Zn, which are present in
354 gasoline type fuels, tire and brake pad wear, oils, lubricants, and grease transport (Trujillo-
355 González *et al.*, 2016).

356 In catchment characterized by soils with very distinct mineralogical properties, a simple
357 qualitative comparison of mid-infrared spectra proved to provide a fast and efficient technique to
358 identify the main sediment sources. In Mexico, Evrard *et al.* (2013) showed that the mid-infrared
359 spectrum of Acrisols was characterized by the dominance of kaolinite in the clay fraction (bands
360 at $3600\text{--}3700\text{ cm}^{-1}$), whereas Andisol spectra were characterized by gibbsite. Similarly, in the
361 French Alps, Poulenard *et al.* (2012) showed that soils developed on gypsum substrates were
362 characterized by absorption bands at 3500 cm^{-1} and in the region between 2370 and 2060 cm^{-1} ,
363 corresponding to CaSO_4 ; whereas soils developed on molasses were characterized by absorption
364 bands at $2430\text{--}2640\text{ cm}^{-1}$ corresponding to calcite (CaCO_3) and absorption bands at $3500\text{--}3700$
365 cm^{-1} corresponding to aluminosilicates. However, Poulenard *et al.* (2012) warned against the
366 application of MIR-PLSR models in catchments characterized by more complex sources of
367 sediment, with variations in soil types and land uses. This may typically be the case in studies
368 discriminating catchment compartments (surface vs. subsurface) as in the current research.

369 As MIR is very sensitive to organic matter, the discrimination of sediment sources with
370 similar organic carbon contents can be difficult if there are no additional differences in mineral
371 composition. Further efforts should be made to combine the information provided by both methods
372 in order to provide estimations of sediment source contributions with a higher precision.

373

374

CONCLUSIONS

375 This study showed the potential of using an alternative sediment fingerprinting method
376 based on mid-infrared (MIR) spectroscopy to quantify sediment source contributions in a
377 subtropical rural catchment of southern Brazil. MIR spectra were comparable in both suspended
378 sediment and potential sources, and 16 spectral features could be identified in all spectra to
379 differentiate them. Sources could be distinguished with this method, although the discrimination

380 between these sources could not be attributed to the detection of specific minerals. The model
381 based on MIR spectra correctly classified $97.5\pm 2.5\%$ of the source samples. The discrimination of
382 cropland and channel banks was possible given their differences in clay mineral contents. In
383 contrast, the similar organic matter content found in both sources complicated their discrimination
384 by the spectroscopic method.

385 When the results of the current research based on MIR spectroscopy are compared to those
386 obtained using other approaches based on geochemistry (Tiecher *et al.*, 2015), ultraviolet-visible
387 (UV-VIS) (Tiecher *et al.*, 2015), and near-infrared (NIR) spectroscopy (Tiecher *et al.*, 2016),
388 results of the current research focusing on MIR spectroscopy showed an overestimation of channel
389 bank contribution and an underestimation of cropland and unpaved road contributions. Moreover,
390 among the spectroscopic approaches, predictions based on the analysis of the MIR region showed
391 the highest difference in source contributions compared to those obtained with the geochemical
392 conventional approach which is considered to provide the 'ground truth'. Mid-infrared
393 spectroscopy signatures were clearly impacted by the low organic carbon content of deep soil
394 horizons, as that found in unpaved road material, resulting in a better discrimination of this source
395 and similar contributions to sediment calculated by geochemical approach. In the future, additional
396 tracers could be used, e.g. fallout radionuclides including ^{137}Cs , to provide further discrimination
397 between surface and subsurface material in order to validate the relevance of the low-cost MIR
398 spectroscopy approach for tracing sediment sources in rural catchments.

399

400

ACKNOWLEDGEMENTS

401 This study was funded by the Brazilian National Council for Scientific and Technological
402 Development (CNPq) and the Foundation for Research Support of the State of Rio Grande do Sul
403 (FAPERGS), and the CAPES-COFECUB project No. 761/12. The authors are also grateful to
404 Clamarion Maier for his assistance during fieldwork.

405

406

REFERENCES

- 407 Argenta DPB, Pante AR, Merten GH. 2001. Evaluation erosivity index of production north-
408 northeast of the state of Rio Grande do Sul. In *Hall of Undergraduate Research: 13. Book*
409 *of Abstracts* UFRGS: Porto Alegre; 37.
- 410 Barros CAP de, Minella JPG, Dalbianco L, Ramon R. 2014. Description of hydrological and
411 erosion processes determined by applying the LISEM model in a rural catchment in
412 southern Brazil. *Journal of Soils and Sediments* **14** (7): 1298–1310 DOI: 10.1007/s11368-
413 014-0903-7
- 414 Brosinsky A, Foerster S, Segl K, Kaufmann H. 2014a. Spectral fingerprinting: sediment source
415 discrimination and contribution modelling of artificial mixtures based on VNIR-SWIR
416 spectral properties. *Journal of Soils and Sediments* **14** (12): 1949–1964 DOI:
417 10.1007/s11368-014-0925-1

- 418 Brosinsky A, Foerster S, Segl K, López-Tarazón JA, Piqué G, Bronstert A. 2014b. Spectral
419 fingerprinting: characterizing suspended sediment sources by the use of VNIR-SWIR
420 spectral information. *Journal of Soils and Sediments* **14** (12): 1965–1981 DOI:
421 10.1007/s11368-014-0927-z
- 422 Cao L, Zhang K, Dai H, Liang Y. 2015. Modeling Interrill Erosion on Unpaved Roads in the
423 Loess Plateau of China. *Land Degradation and Development* **26** (8): 825–832 DOI:
424 10.1002/ldr.2253
- 425 Chang C, Laird DA, Mausbach MJ, Hurburgh CR. 2001. Near-infrared reflectance spectroscopy-
426 principal components regression analyses of soil properties. *Soil Science Society of America*
427 *Journal* **65** (2): 480–490 DOI: 10.2136/sssaj2001.652480x
- 428 Collins A., Walling D. 2002. Selecting fingerprint properties for discriminating potential
429 suspended sediment sources in river basins. *Journal of Hydrology* **261** (1-4): 218–244 DOI:
430 10.1016/S0022-1694(02)00011-2
- 431 Collins AL, Williams LJ, Zhang YS, Marius M, Dungait JAJ, Smallman DJ, Dixon ER,
432 Stringfellow A, Sear DA, Jones JI, et al. 2014. Sources of sediment-bound organic matter
433 infiltrating spawning gravels during the incubation and emergence life stages of salmonids.
434 *Agriculture, Ecosystems and Environment* **196**: 76–93 DOI: 10.1016/j.agee.2014.06.018
- 435 Comino JR, Brings C, Lassu T, Iserloh T, Senciales JM, Martínez Murillo JF, Ruiz Sinoga JD,
436 Seeger M, Ries JB. 2015. Rainfall and human activity impacts on soil losses and rill erosion
437 in vineyards (Ruwer Valley, Germany). *Solid Earth* **6** (3): 823–837 DOI: 10.5194/se-6-823-
438 2015
- 439 Cooper RJ, Rawlins BG, Lézé B, Krueger T, Hiscock KM. 2014. Combining two filter paper-
440 based analytical methods to monitor temporal variations in the geochemical properties of
441 fluvial suspended particulate matter. *Hydrological Processes* **28** (13): 4042–4056 DOI:
442 10.1002/hyp.9945
- 443 D’Haen K, Verstraeten G, Degryse P. 2012. Fingerprinting historical fluvial sediment fluxes.
444 *Progress in Physical Geography* **36** (2): 154–186 DOI: 10.1177/0309133311432581
- 445 Davis CM, Fox JF. 2009. Sediment Fingerprinting: Review of the Method and Future
446 Improvements for Allocating Nonpoint Source Pollution. *Journal of Environmental*
447 *Engineering* **135** (7): 490–504 DOI: 10.1061/(ASCE)0733-9372(2009)135:7(490)
- 448 Didoné EJ, Minella JPG, Merten GH. 2015. Quantifying soil erosion and sediment yield in a
449 catchment in southern Brazil and implications for land conservation. *Journal of Soils and*
450 *Sediments* DOI: 10.1007/s11368-015-1160-0
- 451 Dodd RJ, Sharpley AN. 2015. Recognizing the role of soil organic phosphorus in soil fertility
452 and water quality. *Resources, Conservation and Recycling* DOI:
453 10.1016/j.resconrec.2015.10.001
- 454 Dodd RJ, McDowell RW, Condon LM. 2014. Is tillage an effective method to decrease
455 phosphorus loss from phosphorus enriched pastoral soils? *Soil and Tillage Research* **135**:
456 1–8 DOI: 10.1016/j.still.2013.08.015
- 457 Erkossa T, Wudneh A, Desalegn B, Taye G. 2015. Linking soil erosion to on-site financial cost:
458 Lessons from watersheds in the Blue Nile basin. *Solid Earth* **6** (2): 765–774 DOI:
459 10.5194/se-6-765-2015
- 460 Evrard O, Poulénard J, Némery J, Ayrault S, Gratiot N, Duvert C, Prat C, Lefèvre I, Bonté P,
461 Esteves M. 2013. Tracing sediment sources in a tropical highland catchment of central
462 Mexico by using conventional and alternative fingerprinting methods. *Hydrological*
463 *Processes* **27** (6): 911–922 DOI: 10.1002/hyp.9421
- 464 Fernández-Getino AP, Hernández Z, Piedra Buena A, Almendros G. 2010. Assessment of the
465 effects of environmental factors on humification processes by derivative infrared
466 spectroscopy and discriminant analysis. *Geoderma* **158** (3-4): 225–232 DOI:
467 10.1016/j.geoderma.2010.05.002
- 468 Haddadchi A, Ryder DS, Evrard O, Olley J. 2013. Sediment fingerprinting in fluvial systems:

469 review of tracers, sediment sources and mixing models. *International Journal of Sediment*
470 *Research* **28** (4): 560–578 DOI: 10.1016/S1001-6279(14)60013-5

471 IUSS Working Group WRB. 2007. *World Reference Base for Soil Resources 2006, first update*
472 *2007*. Food and Agriculture Organization of the United Nations – FAO: Rome, Italy.

473 Koiter a. J, Owens PN, Petticrew EL, Lobb D a. 2013. The behavioural characteristics of
474 sediment properties and their implications for sediment fingerprinting as an approach for
475 identifying sediment sources in river basins. *Earth-Science Reviews* **125**: 24–42 DOI:
476 10.1016/j.earscirev.2013.05.009

477 Legout C, Poulenard J, Nemery J, Navratil O, Grangeon T, Evrard O, Esteves M. 2013.
478 Quantifying suspended sediment sources during runoff events in headwater catchments
479 using spectroradiometry. *Journal of Soils and Sediments* **13** (8): 1478–1492 DOI:
480 10.1007/s11368-013-0728-9

481 Madejová J, Balan E, Petit S. 2011. Application of vibrational spectroscopy to the
482 characterization of phyllosilicates and other industrial minerals. In *Advances in the*
483 *Characterization of Industrial Minerals*, Christidis GE (ed.). European Mineralogical Union
484 and the Mineralogical Society of Great Britain and Ireland: London, UK; 171–226.

485 Magnusson M, Heimann K, Ridd M, Negri AP. 2013. Pesticide contamination and phytotoxicity
486 of sediment interstitial water to tropical benthic microalgae. *Water research* **47** (14): 5211–
487 21 DOI: 10.1016/j.watres.2013.06.003

488 Maier C. 2013. Variabilidade intra-evento da origem das fontes de sedimentos em uma bacia
489 hidrográfica rural (Intra-event variability of sources from sediment basin in a rural).2013.
490 124 f. Thesis (PhD in Water Resources and Sanitation) – Universidade Federal do Rio
491 Grande do Sul, Porto Alegre.

492 Martínez-Carreras N, Krein A, Gallart F, Iffly JF, Pfister L, Hoffmann L, Owens PN. 2010a.
493 Assessment of different colour parameters for discriminating potential suspended sediment
494 sources and provenance: A multi-scale study in Luxembourg. *Geomorphology* **118** (1-2):
495 118–129 DOI: 10.1016/j.geomorph.2009.12.013

496 Martínez-Carreras N, Krein A, Udelhoven T, Gallart F, Iffly JF, Hoffmann L, Pfister L, Walling
497 DE. 2010b. A rapid spectral-reflectance-based fingerprinting approach for documenting
498 suspended sediment sources during storm runoff events. *Journal of Soils and Sediments* **10**
499 (3): 400–413 DOI: 10.1007/s11368-009-0162-1

500 Martínez-Carreras N, Udelhoven T, Krein A, Gallart F, Iffly JF, Ziebel J, Hoffmann L, Pfister L,
501 Walling DE. 2010c. The use of sediment colour measured by diffuse reflectance
502 spectrometry to determine sediment sources: Application to the Attert River catchment
503 (Luxembourg). *Journal of Hydrology* **382** (1-4): 49–63 DOI: 10.1016/j.jhydrol.2009.12.017

504 McBratney AB, Minasny B, Viscarra Rossel R. 2006. Spectral soil analysis and inference
505 systems: A powerful combination for solving the soil data crisis. *Geoderma* **136** (1-2): 272–
506 278 DOI: 10.1016/j.geoderma.2006.03.051

507 Merten GH, Araújo AG, Biscaia RCM, Barbosa GMC, Conte O. 2015. No-till surface runoff and
508 soil losses in southern Brazil. *Soil and Tillage Research* **152**: 85–93 DOI:
509 10.1016/j.still.2015.03.014

510 Minella JPG, Merten GH, Clarke RT. 2009a. Método ‘fingerprinting’ para identificação de
511 fontes de sedimentos em bacia hidrográfica rural. *Revista Brasileira de Engenharia*
512 *Agrícola e Ambiental* **13** (5): 633–638 DOI: 10.1590/S1415-43662009000500017

513 Minella JPG, Merten GH, Walling DE, Reichert JM. 2009b. Changing sediment yield as an
514 indicator of improved soil management practices in southern Brazil. *Catena* **79** (3): 228–
515 236 DOI: 10.1016/j.catena.2009.02.020

516 Minella JPG, Walling DE, Merten GH. 2008. Combining sediment source tracing techniques
517 with traditional monitoring to assess the impact of improved land management on
518 catchment sediment yields. *Journal of Hydrology* **348** (3-4): 546–563 DOI:
519 10.1016/j.jhydrol.2007.10.026

- 520 Minella JPG, Walling DE, Merten GH. 2014. Establishing a sediment budget for a small
521 agricultural catchment in southern Brazil, to support the development of effective sediment
522 management strategies. *Journal of Hydrology* **519**: 2189–2201 DOI:
523 10.1016/j.jhydrol.2014.10.013
- 524 Navarro-Hevia J, Lima-Farias TR, de Araújo JC, Osorio-Peláez C, Pando V. 2016. Soil Erosion
525 in Steep Road Cut Slopes in Palencia (Spain). *Land Degradation and Development* **27** (2):
526 190–199 DOI: 10.1002/ldr.2459
- 527 Poulenard J, Dorioz J-M, Elsass F. 2008. Analytical Electron-Microscopy Fractionation of Fine
528 and Colloidal Particulate-Phosphorus in Riverbed and Suspended Sediments. *Aquatic
529 Geochemistry* **14** (3): 193–210 DOI: 10.1007/s10498-008-9032-5
- 530 Poulenard J, Legout C, Némery J, Bramorski J, Navratil O, Douchin a., Fanget B, Perrette Y,
531 Evrard O, Esteves M. 2012. Tracing sediment sources during floods using Diffuse
532 Reflectance Infrared Fourier Transform Spectrometry (DRIFTS): A case study in a highly
533 erosive mountainous catchment (Southern French Alps). *Journal of Hydrology* **414-415**:
534 452–462 DOI: 10.1016/j.jhydrol.2011.11.022
- 535 Poulenard J, Perrette Y, Fanget B, Quetin P, Trevisan D, Dorioz JM. 2009. Infrared spectroscopy
536 tracing of sediment sources in a small rural watershed (French Alps). *The Science of the
537 Total Environment* **407** (8): 2808–19 DOI: 10.1016/j.scitotenv.2008.12.049
- 538 Pulley S, Rowntree K. 2015. The use of an ordinary colour scanner to fingerprint sediment
539 sources in the South African Karoo. *Journal of environmental management* **165**: 253–262
540 DOI: 10.1016/j.jenvman.2015.09.037
- 541 Reeves JB. 2010. Near- versus mid-infrared diffuse reflectance spectroscopy for soil analysis
542 emphasizing carbon and laboratory versus on-site analysis: Where are we and what needs to
543 be done? *Geoderma* **158** (1-2): 3–14 DOI: 10.1016/j.geoderma.2009.04.005
- 544 Scheinost AC, Chavernas A, Barrón V, Torrent J. 1998. Use and limitations of second-derivative
545 diffuse reflectance spectroscopy in the visible to near-infrared range to identify and quantify
546 Fe oxide minerals in soils. *Clays and Clay Minerals* **46** (5): 528–536 DOI:
547 10.1346/CCMN.1998.0460506
- 548 Seutloali KE, Beckedahl HR. 2015. Understanding the factors influencing rill erosion on
549 roadcuts in the south eastern region of South Africa. *Solid Earth* **6** (2): 633–641 DOI:
550 10.5194/se-6-633-2015
- 551 Soil Survey Division Staff. 1993. Examination and description of soils. In *Soil Survey
552 Manual* Soil Conservation Service. U.S. Department of Agriculture Handbook 18; 46–155.
553 DOI: 10.1097/00010694-195112000-00022
- 554 Soriano-Disla JM, Janik LJ, Viscarra Rossel R a, Macdonald LM, McLaughlin MJ. 2014. The
555 Performance of Visible, Near-, and Mid-Infrared Reflectance Spectroscopy for Prediction
556 of Soil Physical, Chemical, and Biological Properties. *Applied Spectroscopy Reviews* **49**
557 (2): 139–186 DOI: 10.1080/05704928.2013.811081
- 558 Taguas EV, Guzmán E, Guzmán G, Vanwalleghem T, Gómez JA. 2015. Characteristics and
559 importance of rill and gully erosion: a case study in a small catchment of a marginal olive
560 grove. *Cuadernos de Investigación Geográfica* **41** (1): 107 DOI: 10.18172/cig.2644
- 561 Terra F da S. 2011. Espectroscopia de reflectância do visível ao infravermelho médio aplicada
562 aos estudos qualitativos e quantitativos de solos (Reflectance spectroscopy from visible to
563 mid-infrared applied for qualitative and quantitative studies of soils).2011. 375 f. Thesis
564 (PhD in Soil Science) – Universidade de São Paulo Escola Superior de Agricultura ‘ Luiz
565 de Queiroz ’, Piracicaba, São Paulo.
- 566 Tiecher T, Caner L, Minella JPG, Bender MA, dos Santos DR. 2016. Tracing sediment sources
567 in a subtropical rural catchment of southern Brazil by using geochemical tracers and near-
568 infrared spectroscopy. *Soil and Tillage Research* **155**: 478–491 DOI:
569 10.1016/j.still.2015.03.001
- 570 Tiecher T, Caner L, Minella JPG, dos Santos DR. 2015. Combining visible-based-color

571 parameters and geochemical tracers to improve sediment source discrimination and
572 apportionment. *The Science of the total environment* **527-528**: 135–49 DOI:
573 10.1016/j.scitotenv.2015.04.103

574 Trujillo-González JM, Torres-Mora MA, Keesstra S, Brevik EC, Jiménez-Ballesta R. 2016.
575 Heavy metal accumulation related to population density in road dust samples taken from
576 urban sites under different land uses. *Science of the Total Environment* **553**: 636–642 DOI:
577 10.1016/j.scitotenv.2016.02.101

578 Verheyen D, Diels J, Kissi E, Poesen J. 2014. The use of visible and near-infrared reflectance
579 measurements for identifying the source of suspended sediment in rivers and comparison
580 with geochemical fingerprinting. *Journal of Soils and Sediments* **14** (11): 1869–1885 DOI:
581 10.1007/s11368-014-0938-9

582 Viscarra Rossel R a., Walvoort DJJ, McBratney a. B, Janik LJ, Skjemstad JO. 2006. Visible,
583 near infrared, mid infrared or combined diffuse reflectance spectroscopy for simultaneous
584 assessment of various soil properties. *Geoderma* **131** (1-2): 59–75 DOI:
585 10.1016/j.geoderma.2005.03.007

586 Viscarra Rossel RA, Behrens T. 2010. Using data mining to model and interpret soil diffuse
587 reflectance spectra. *Geoderma* **158** (1-2): 46–54 DOI: 10.1016/j.geoderma.2009.12.025

588 Walling DE, Woodward JC. 1995. Tracing sources of suspended sediment in river basins: a case
589 study of the River Culm, Devon, UK. *Marine and Freshwater Research* **46** (1): 327–336
590 DOI: 10.1071/MF9950327

591 Xie HT, Yang XM, Drury CF, Yang JY, Zhang XD. 2011. Predicting soil organic carbon and
592 total nitrogen using mid- and near-infrared spectra for Brookston clay loam soil in
593 Southwestern Ontario, Canada. *Canadian Journal of Soil Science* **91** (1): 53–63 DOI:
594 10.4141/cjss10029

595 Yahia D, Elsharkawy EE. 2014. Multi pesticide and PCB residues in Nile tilapia and catfish in
596 Assiut city, Egypt. *The Science of the total environment* **466-467**: 306–14 DOI:
597 10.1016/j.scitotenv.2013.07.002

598 Yang H, Mouazen AM. 2012. Vis/near and mid-infrared spectroscopy for predicting soil N and
599 C at a farm scale. In *Infrared Spectroscopy-Life and Biomedical Sciences*, Theophanides T
600 (ed.).Intech Press: Rijeka, Croatia; 185–210.

601
602

603

Table 1. Characteristics of the absorption features detected by MIR spectroscopy.

Spectral feature	Wavenumber (cm ⁻¹)	Wavenumber according to the literature (cm ⁻¹)	Soil constituent	Functional group	MIR mode
1	3695	3695 ^a	Kt	O–H	v _{1a}
2	3620	3620 ^a	Kt	O–H	v _{1b}
		3620 ^a	Sm	O–H	v ₁
		3620 ^a	Mc	O–H	v ₁
3	2930	2930 ^a	OC (aromatic)	C–H	v ₃
4	2850	2850 ^a	OC (aliphatic)	C–H	v ₁
5	1990	1975 ^b	Qz	Si–O	v
6	1870	1867 ^b	Qz	Si–O	v
7	1785	1790 ^b	Qz	Si–O	v
8	1630	1628 ^b	Kt, Sm, Mc, HIV	O–H	δ
		1628 ^b	Qz	Si–O	v
9	1530	1527 ^b	Qz	Si–O	v
		1525 ^c	OC (aromatic)	C=C	v
10	1340	1527 ^b	Qz	Si–O	v
		1350 ^c	OC (aliphatic)	C–H	v
11	1160	1157 ^b	OC (polysaccharide)	C–O	v
		1157 ^b	OC (aliphatic)	C–OH	v
		1157 ^b	Kt, Sm, Mc, HIV	O–Al–OH	δ
12	1115	1111 ^b	Kt, Sm, Mc, HIV	Si–O–Si	v
		1111 ^b	Gb	Al–O–OH	δ
13	1020	1018 ^b	Kt, Sm, Mc, HIV	Si–O–Si	v ₅
14	915	915 ^a	Kt	Al–OH	δ
		915 ^a	Sm	Al–OH	δ _a
15	808	814 ^b	Qz	Si–O	v
		814 ^b	Kt, HIV, Gb	Al–OH	δ
16	698	702 ^b	Kt, Sm, Mc, HIV	Si–O	v

604 Kt, kaolinite; Sm, smectite; Mc, micas; HIV, hydroxy-interlayered vermiculite; Gb, gibbsite; Qz, quartz; OC, organic compounds.

605 ^a Viscarra Rossel and Behrens (2010)606 ^b Terra (2011)607 ^c Yang and Mouazen (2012)

608

609 **Table 2.** Results of the discriminant function analysis and prediction error for the MIR spectroscopy
 610 approach.

DFA parameters	Source	Value
F-values (F critical = 2.4)	SC vs. UR	27.9
	SC vs. CF	17.7
	UR vs. CF	28.6
p-levels	SC vs. UR	2.2E-11
	SC vs. CF	6.5E-09
	UR vs. CF	1.6E-11
Squared Mahalanobis distances	SC vs. UR	38.7
	SC vs. CF	18.4
	UR vs. CF	29.7
	Average	28.9
Source samples correctly classified (%)	SC	100
	UR	100
	CF	95
	Average	97.5
Uncertainty associated with source discrimination (%)	SC	0.311
	UR	0.751
	CF	6.322
	Average	3.426
Prediction error (%)	SC	5.1
	UR	2.8
	CF	5.9
	Average	4.6

612
 613 **Table 3.** Predictive performance of the MIR-PLSR models based on MIR spectroscopy.

Sediment source	NC	R _{adj}	RMSEC	RMSEP	RMSECV	RPD
Crop fields	4	0.9903	2.1	4.7	2.9	10.0
Unpaved roads	4	0.9978	1.2	2.1	1.5	19.8
Stream channels	4	0.9929	1.6	3.9	2.3	12.4

614 NC, number of components used in the MIR-PLSR model; R_{adj}, coefficient of determination; RMSEC, root mean square error of
 615 calibration; RMSEP, root mean square error of prediction; RMSECV, root mean square error of cross-validation; RPD, ratio
 616 between the standard deviation and RMSECV.

617
 618 **Table 4.** Linear correlation between the sediment source contributions predicted by sediment fingerprinting
 619 techniques based on MIR spectroscopy, NIR spectroscopy (Tiecher *et al.*, 2016), UV-VIS spectroscopy
 620 and elemental geochemistry (Tiecher *et al.*, 2015).

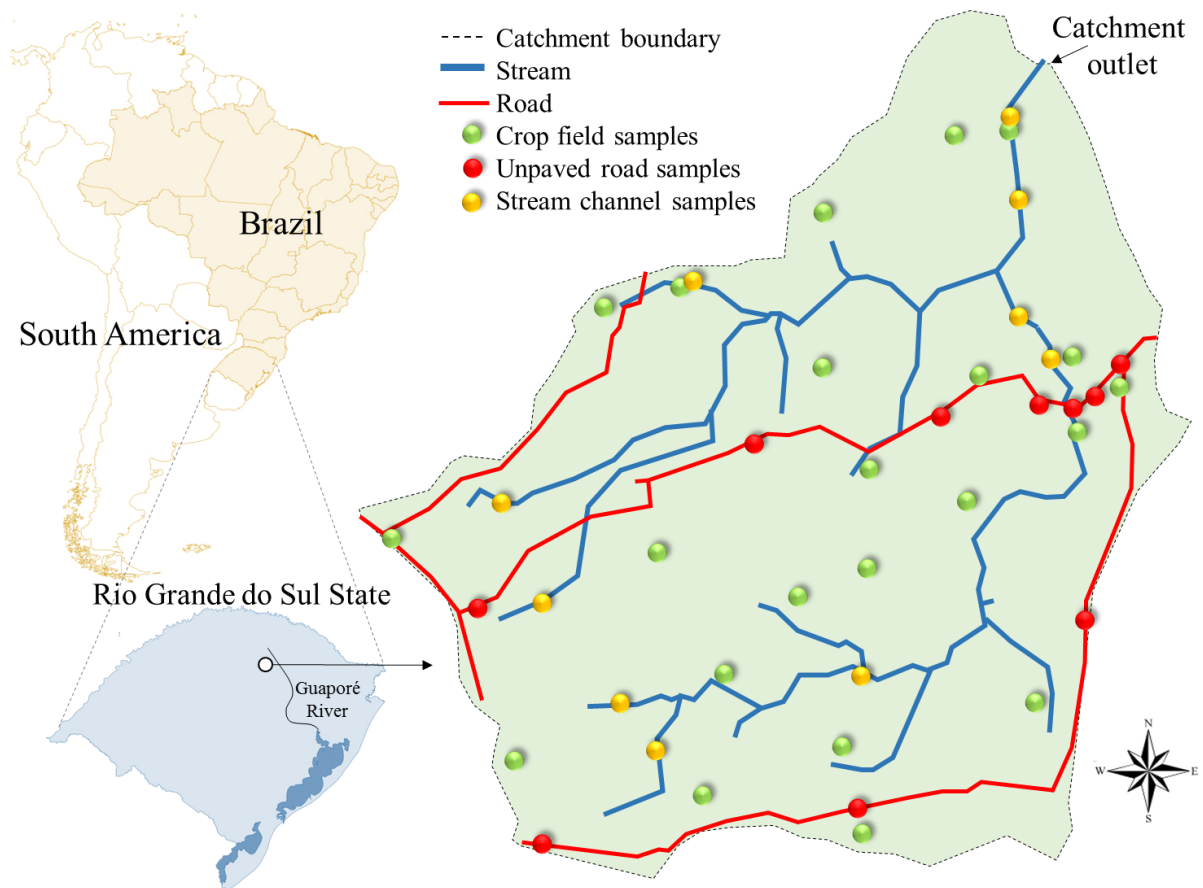
Sediment source/method	MIR-spectroscopy		Geochemistry ^a		UV-VIS-spectroscopy ^a	
	<i>r</i>	<i>p</i> -value	<i>r</i>	<i>p</i> -value	<i>r</i>	<i>p</i> -value
<i>Cropland</i>						
Geochemistry ^a	0.57	0.001				
UV-VIS-spectroscopy ^a	0.43	0.019	0.31	0.098		
NIR-spectroscopy ^b	0.04	0.826	0.01	0.962	-0.44	0.018
<i>Channel bank</i>						
Geochemistry ^a	-0.01	0.939				
UV-VIS-spectroscopy ^a	0.31	0.098	-0.22	0.253		
NIR-spectroscopy ^b	0.07	0.701	0.22	0.251	0.37	0.049
<i>Unpaved road</i>						
Geochemistry ^a	0.30	0.108				
UV-VIS-spectroscopy ^a	0.61	0.001	0.59	0.001		
NIR-spectroscopy ^b	0.54	0.003	-0.07	0.718	0.23	0.230

621 Values in **bold** indicate significant correlation between source contributions estimated by both methods at $P < 0.05$

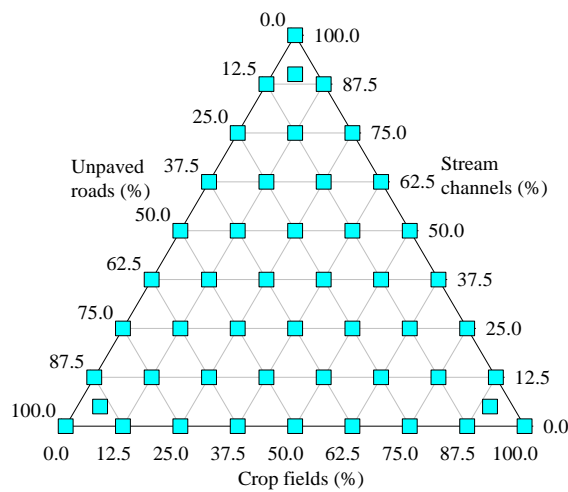
622 ^a Tiecher *et al.* (2015)

623 ^b Tiecher *et al.* (2016)

624

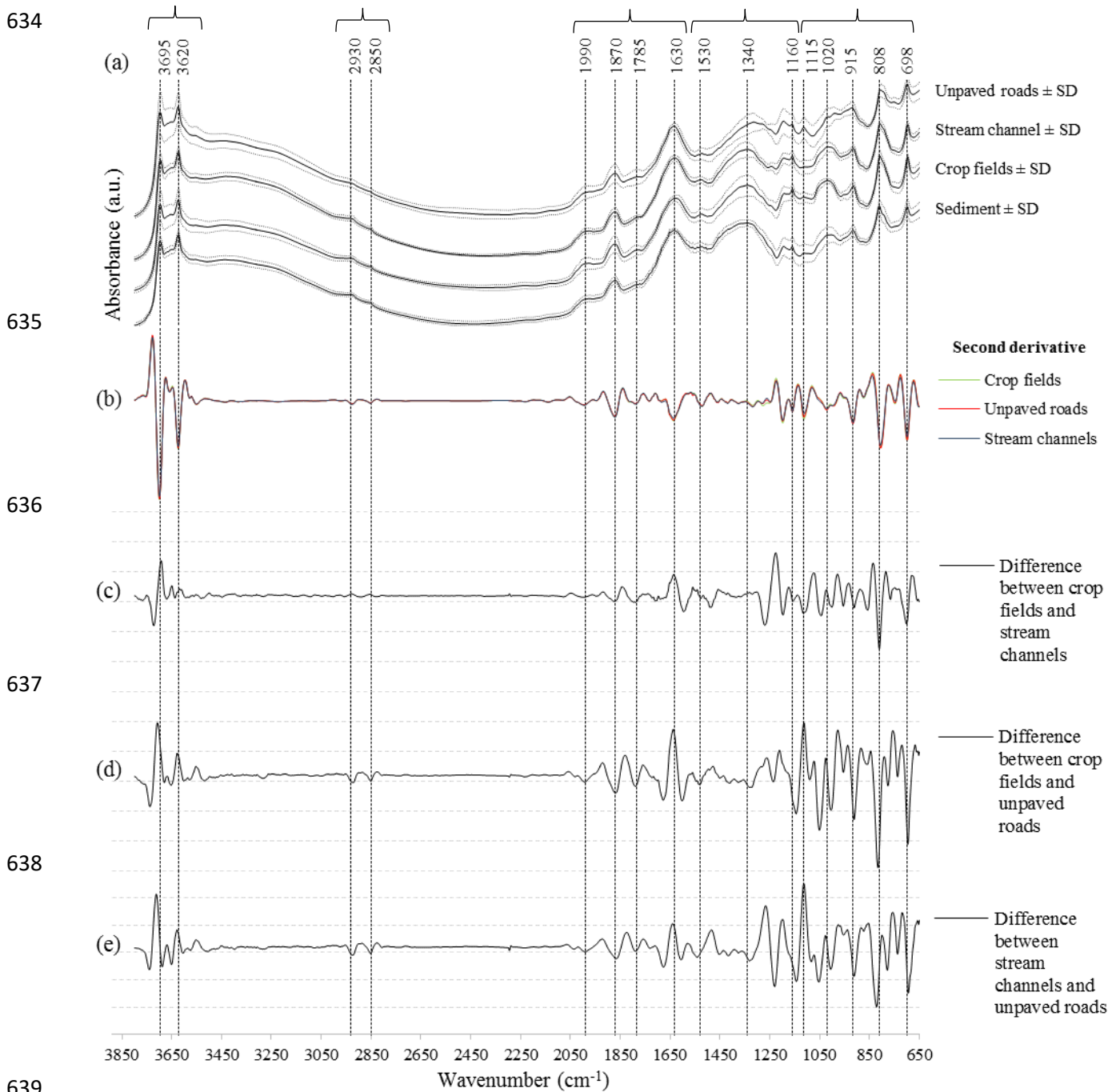


625
 626 **Fig. 1.** Location of the Arvorezinha catchment in Southern Brazil, and location of the potential
 627 sediment source sampling sites.
 628



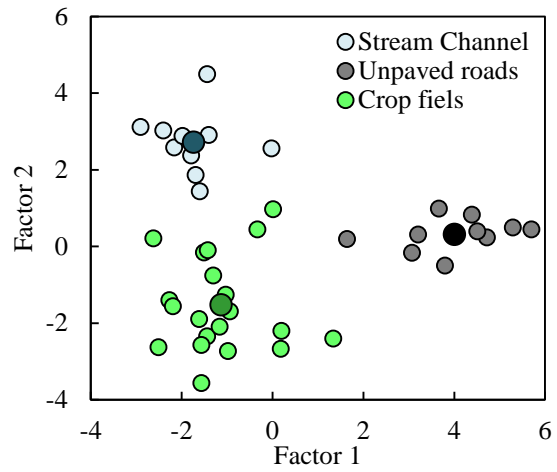
629
 630 **Fig. 2.** Ternary diagram showing the composition of the experimental mixtures prepared in the
 631 laboratory for the MIR-PLSR model calibration.

632
633
634



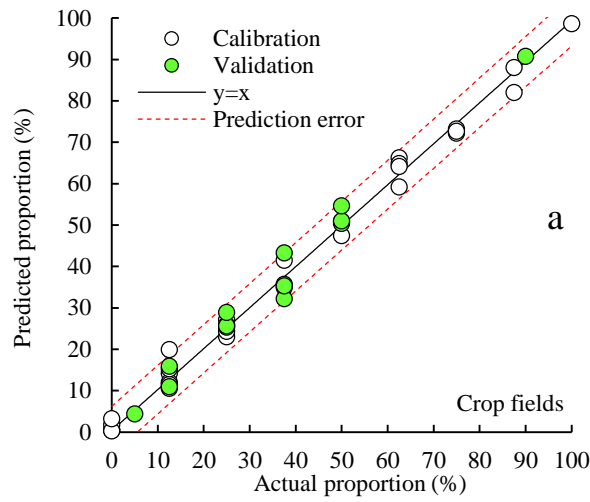
639
640
641
642
643

Fig. 3. Mean MIR spectra of the main sediment sources (unpaved road [UR], stream channel [SC], and crop field [CF]) and suspended sediment (a), second-derivative of the UR, SC, and CF (b), difference between CF and SC (c), difference between CF and UR (d), and difference between SC and UR (e).

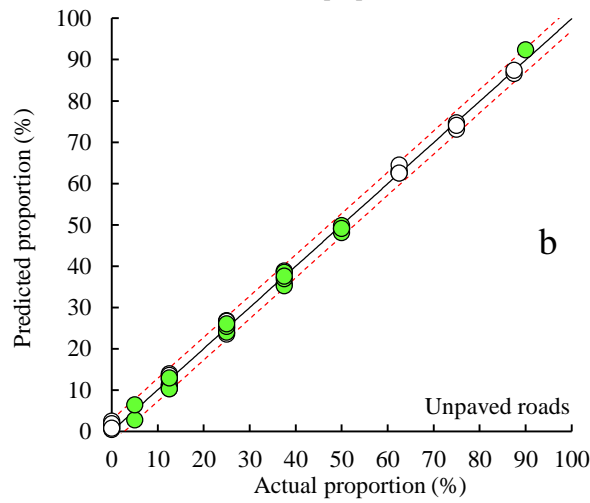


644
 645 **Fig. 4.** Two-dimensional scatter plot of the first and second discriminant functions derived from
 646 stepwise discriminant function analysis (DFA) applied to MIR spectroscopy. Larger symbols
 647 represent the centroids of each source.
 648

649



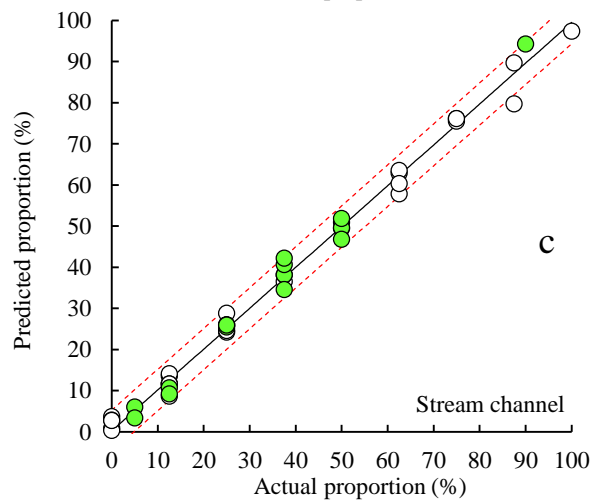
650

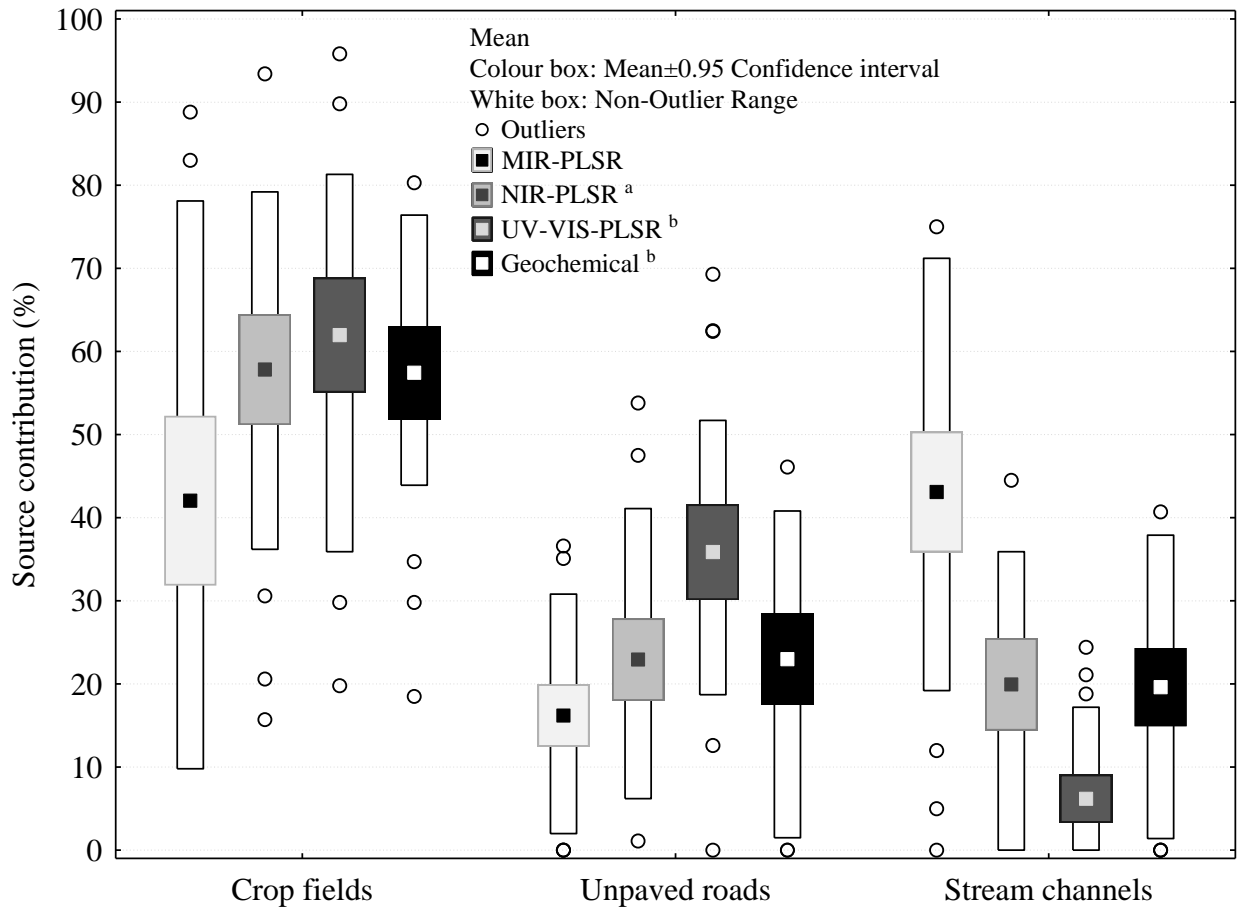


651

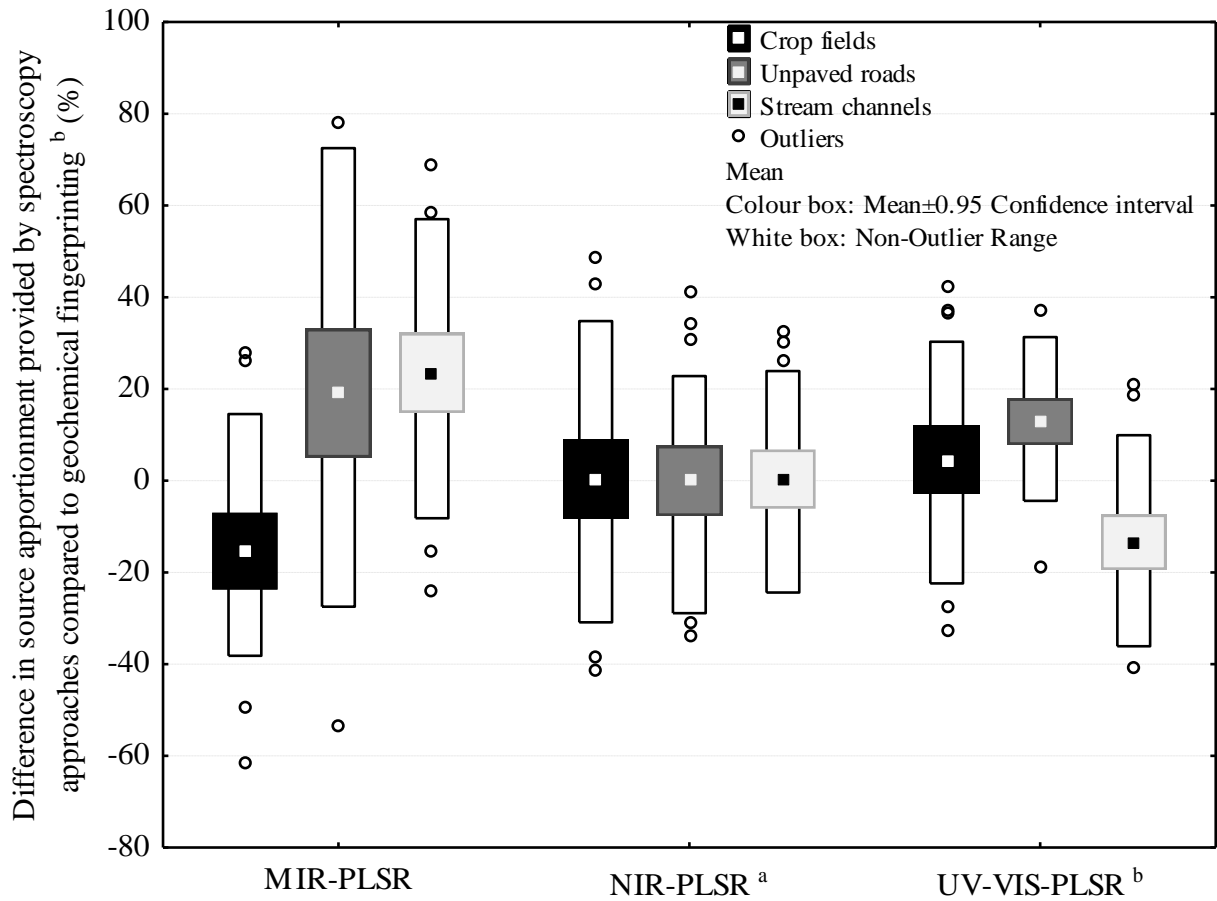
652 **Fig. 5.** Relationship between actual proportions of sediment sources and those calculated using
653 MIR-PLSR models in experimental mixtures for crop fields (a), unpaved roads (b), and
654 stream channels (c). Red dashed lines provide the 95-% confidence limits (95%).

655





656
 657 **Fig. 6.** Box plot of the sediment source contributions for the 29 suspended sediment samples
 658 collected at the Arvorezinha catchment outlet, estimated by MIR spectroscopy (this study), NIR-
 659 spectroscopy (a – Tiecher *et al.*, 2016), UV-VIS spectroscopy and conventional sediment
 660 fingerprinting approach based on elemental geochemistry (b – Tiecher *et al.*, 2015).
 661
 662



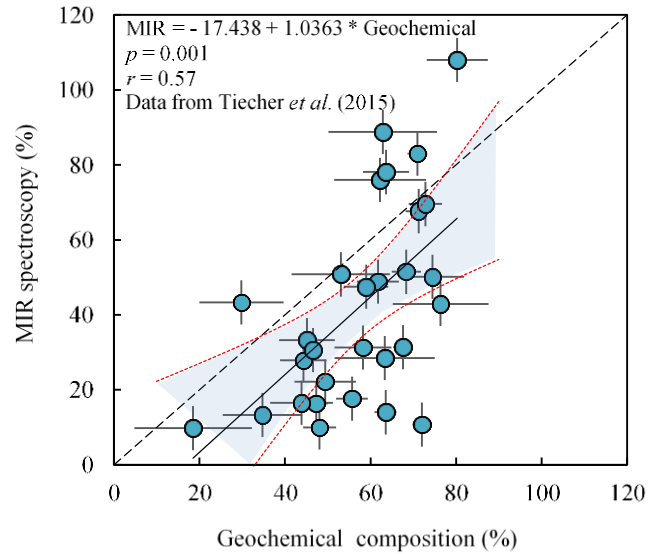
663
 664 **Fig. 7.** Box plot of the difference in source apportionment provided by spectroscopy approaches
 665 compared to geochemical fingerprinting (Tiecher *et al.*, 2015) for the 29 suspended sediment
 666 samples collected at the Arvorezinha catchment.

667 ^a Tiecher *et al.* (2016)

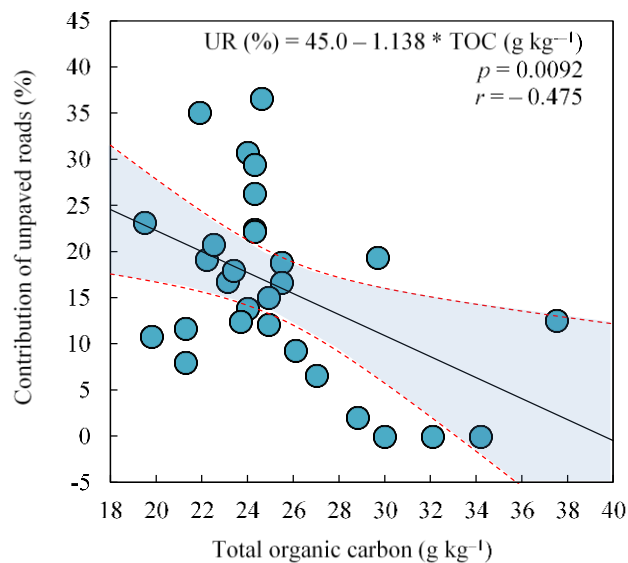
668 ^b Tiecher *et al.* (2015)

669

670



671
 672 **Fig. 8.** Comparison of the crop field contributions to sediment predicted by the conventional
 673 sediment fingerprinting method based on elemental geochemistry (Tiecher *et al.*, 2015) and those
 674 predicted by the partial least-squares regression model based on MIR spectroscopy. Error bars
 675 correspond to the estimated error of prediction for each method. The dashed line represents the 1:1
 676 line. Red dotted lines provide the 95-% confidence limits.
 677



678
 679 **Fig. 9.** Relationship between the unpaved roads contributions to sediment predicted by the partial
 680 least-squares regression model based on MIR spectroscopy and the total organic carbon content in
 681 sediment. The red dashed lines provide the 95-% confidence limits.
 682